

Molecular Dynamics Simulations of the Cytolytic Toxin Cyt1A in Solution

Jun Xie[†], Peter Butko[‡], and Dexuan Xie^{† 1}

[†]*Department of Mathematical Sciences
University of Wisconsin, Milwaukee, WI 53211*

[‡]*Department of Chemistry and Biochemistry
University of Southern Mississippi, Hattiesburg, MS 39406*

Abstract Cytolytic toxin Cyt1A from *Bacillus thuringiensis* var. *israelensis* is used for an environmentally friendly insecticide, but its mode of action has not been clearly established. The reasons for this include the lack of experimentally determined structure of Cyt1A in solution. If the membrane-bound Cyt1A is in the molten-globule state as suggested, computer simulation may become the only tool for studying the structure and function of Cyt1A. As a first step in computer simulations of Cyt1A, in this paper, an initial molecular structure of Cyt1A is generated by a homology modeling. It is then refined and simulated in solution by both molecular potential energy minimizations and molecular dynamics. The regions of the toxin that manifest higher conformational flexibility are identified. The predicted structure is validated and used to create a mutated Cyt1A.

1 Introduction

The cytolytic toxin Cyt1A belongs to a family of toxins produced by *Bacillus thuringiensis* var. *israelensis* and some other subspecies. Many of these toxins, commonly known as Bt toxins (from the initials of the bacteria), are used in environmentally

¹Address correspondence to Dexuan Xie, Department of Mathematical Sciences, University of Wisconsin, Milwaukee, WI 53211. Email: dxie@uwm.edu. Submitted to *Biomacromolecules*, a journal of the American Chemical Society, September 2004.

friendly insecticide preparations. Despite the wide use, the mode of action of Cyt toxins has not been unequivocally established [1]. In vivo, Cyt toxins kill larvae of mosquitoes and blackflies and synergistically enhance toxicity of other Bt toxins towards larvae of other insects [2, 3]. In vitro, Cyt toxins destroy not only insect or mammalian cells, but also model lipid membranes [4]. The latter fact indicates that, at least in vitro, the toxin does not require a specific protein receptor and interacts directly with lipids. What happens after the initial binding between the toxin and membrane is a matter of dispute. One hypothesis claims that the toxin inserts in the lipid bilayer and assembles into a channel or pore [5, 6] and the other states that the toxin aggregates into non-stoichiometric structures on the membrane and acts more or less as a detergent [1, 7]. While there has been at least one attempt to visualize the hexameric pore directly [8], other evidence indicates that the membrane-bound toxin assumes an open irregular conformation similar to molten globule [7, 9]. If the latter is true it is hard to imagine a stable, protein-lined pore, which usually requires a very definite structure of the molecules forming the pore. Furthermore, molten globule is very dynamic, with secondary structural elements preserved, but no long-distance order. Therefore it might be impossible to determine the conformation of the membrane-bound Cyt1A experimentally and the only possible recourse would be to use computer simulation.

This paper represents our initial work, in which we first obtained an initial molecular structure of Cyt1A by using a homology modeling based on the crystallographic structure of a homologous toxin Cyt2A [10]. After refining the initial structure by minimizing the molecular potential energy, we studied the evolution of the refined toxin structure by molecular dynamics (MD) simulations in solution. MD generates a realistic picture of atomic or segmental motions within the three dimensional (3D) molecular structure of Cyt1A. With the ascertained Cyt1A conformation in solution, we will include the lipid membrane in the next phase of simulation in order to gain information on conformational changes in the toxin during interaction with lipid, which may significantly contribute to the current dispute on the Cyt1A's mode of action.

2 Materials and Methods

Our MD simulations were carried out by using a widely-used biomolecular simulation program package - CHARMM [11] (version 29) - on one R14000 processor of the SGI Origin 300 computer at the University of Wisconsin-Milwaukee. The modeled system contained one molecule of Cyt1A and a large number of water molecules. Cyt1A consists of 249 amino-acid residues with 3846 atoms. The standard cubic water block of CHARMM, with dimensions $15.6\text{\AA} \times 15.6\text{\AA} \times 15.6\text{\AA}$ and containing 125 water molecules, was used to build the cubic box at the start of the simulation. Periodic boundary conditions were employed in order to eliminate the boundary problem of the cubic water box and also to make the simulation of bulk water more manageable. The periodic boundary conditions can also enable the simulation to be performed with a relatively small number of atoms, each of which exerts and experiences forces as though it was in a bulk solution. The coordinates of the image particles in the surrounding boxes are related to those in the primary box by simple translations. Forces on the primary atoms are calculated from atoms within the same box as well as in the image box.

One important work in carrying out MD simulations is to set up a good initial molecular structure of the molecular system. Since the sequence of Cyt1A is very similar to that of Cyt2A [1], an initial molecular structure of Cyt1A was obtained in Figure 2(A) by a homology modeling based on the crystal structure of the homologous toxin Cyt2A. This work was done by using the protein structure homology-modeling server Swiss-Model [13] and the Swiss-PdbViewer, a graphic interface program package (<http://us.expasy.org/spdbv/>). The crystal structure of Cyt2A was found in the protein databank (<http://www.rcsb.org/pdb/>) with the entry name 1CBY.

As in Cyt2A, the initial structure of Cyt1A contains a peculiar N-terminal tail (residues 1-25), which presumably participates in dimerization of the protoxin in solution. This part of the molecule is cleaved off during the proteolytic activation of the protoxin into the fully active toxin [10]. Therefore, we felt justified to reduce the system size by not including the tail in our first period of MD simulation. As a

result, the activated Cyt1A toxin was completely immersed in a water box with each side 77.8 Å long, containing 15625 water molecules. After a 140 ps simulation, we attached the N-terminus manually, and placed the complete molecule of Cyt1A into a rectangular prism with dimensions 70.9Å×70.0Å×83.8Å, containing 11643 water molecules. We then continued the MD simulation for additional 820 ps.

We used the CHARMM residual topology and parameter files, “top_all22_prot.inp” and “par_all22_prot.inp”, to define protein residues and the force constants, equilibrium geometries, van der Waals radii, and other data needed for calculating the values of molecular potential energy function. In CHARMM, the potential energy function is defined as a sum of the bond length, bond angle, dihedral, improper dihedral, electrostatic, and van der Waals potential energy terms. See [12] for details on the definitions of these potential terms.

The initial structure generated by Swiss-Model was refined by molecular potential energy minimizations in two steps. In the first step, to save the cost of computation, the structure of Cyt1A was refined in vacuum by a combination of two CHARMM minimization methods: the steepest descent (SD) method and the adopted basis Newton-Raphson (ABNR) method. SD was first run for 10000 iteration steps, followed by the ABNR until a minimization termination rule was satisfied. In the second step, the refined structure from the first step was placed into the center of the water box for further refinement by SD for 50000 steps and ABNR until the termination rule was satisfied, which required that the Euclidean norm of the gradient vector of the potential energy function be less than or equal to 0.001 kcal/(mol·Å).

With the energy-minimized conformation as the starting point, MD simulations were carried out in three stages: the heating stage, the equilibrium stage, and the quenching stage. In the heating stage, random velocities were generated according to the Gaussian distribution appropriate for a given low temperature. The equilibration was achieved by allowing the system to evolve spontaneously for a period of time until the average temperature and structure remain stable. In the quenching stage, the equilibrated temperature was gradually reduced back to zero. Quenching is

essentially a form of potential energy minimization, utilizing molecular dynamics to slowly remove all the kinetic energies from the system. The Leapfrog Verlet integrator with a timestep of 0.001 ps was used in our MD simulations. The bond-lengths of all water molecules were restrained. The non-bonded pair list was updated every 25 steps. Data were saved every 0.1 ps. Each 200 ps dynamics calculation took about 560 hours on one 600 MHz R14000 processor of the SGI Origin 300. We first ran the MD simulation of the activated toxin without the N-terminus for a total of 140 ps, and then with the full protoxin for a total of 820 ps.

In the heating stage, the system temperature increased from 0 K to 300 K in 20,000 steps (i.e., 20 ps). In the equilibrium stage, the system temperature was kept as a constant of 300 K. The energy changes of the Cyt1A-water system in the three stages of the MD simulation are shown in Figure 1A. It can be seen that the total energy of the system was constant at about -8.16×10^4 kcal/mol, the kinetic energy about 3.37×10^4 kcal/mol and the potential energy about -11.53×10^4 kcal/mol. Throughout the equilibrium stage, the MD energy fluctuations were too small to be significant (Figure 1B).

Figure 1

3 Results and Discussions

3.1 Predicted molecular structures of Cyt1A by potential energy minimization

Figure 2 displays the initial structure of Cyt1A predicted by Swiss-Model, the structure refined by potential energy minimization, and a comparison between the refined structure and the initial structure in Plots A, B and C, respectively. It shows that the energy minimization has caused non-negligible changes in the predicted structure.

Figure 2

Table 1 lists the energy changes ΔE produced by the minimization, where ΔE is the difference between the minimized energy and the initial energy. It shows that both in vacuum and in water, the energy minimization has reduced the potential energy of the Cyt1A system sharply, and the largest contribution to the energy decrease

Table 1

during minimization comes from the electrostatics. In this context, it is interesting to mention the following two recent experimental observations on the effect of high ionic strength on Cyt1A:

- Increase of salt concentration from 0 to 150 mM caused some changes in Cyt1A conformation, as reported by tryptophan fluorescence [14].
- Binding of the toxin to the lipid was inhibited by high ionic strength [7].

These two observations indicate that electrostatic forces participate both in stabilization of the Cyt1A structure in solution and in the toxin’s interaction with lipid. Our results from the energy minimization are consistent with that notion and we hope that future simulations with the lipid present will provide further support.

3.2 Predicted secondary structure elements of Cyt1A

Figure 3 compares the three secondary structure elements of Cyt1A generated by homology modeling, potential energy minimization, and MD, respectively. Here, stars denote residues in beta strands, and circles denote residues in alpha helices. It shows that the three secondary structures are similar and in a general agreement with the published predicted secondary structure [1]. The only minor discrepancies are that β strand 3 appears to have broken into two in the current simulation and the lack of the short β strand 6a, which was tentatively postulated in [1]. These small changes do not warrant reevaluation of the previously published predicted structure and have no consequence for the discussion of the Cyt1As mode of action.

Figure 3

3.3 Structure changes by MD

In order to illustrate the nature and magnitude of the displacements caused by MD simulations, we introduce the following formula to calculate the values of RMSD (Root Mean Square Deviation) as a function of time t :

$$RMSD(t) = \sqrt{\frac{1}{N} \sum_{i=1}^N [(x_i^t - x_i^I)^2 + (y_i^t - y_i^I)^2 + (z_i^t - z_i^I)^2]} \quad , \quad (1)$$

where (x_i^I, y_i^I, z_i^I) and (x_i^t, y_i^t, z_i^t) denote the positions of atom i in the initial step of MD and in the t -th step of MD, respectively, and N is the total number of atoms in the molecule. The units of RMSD are Angstroms. We computed the values of $RMSD(t)$ for Cyt1A every 0.2 ps in the period of MD simulation time from 0 to 420 ps, and plotted them in Figure 4A. From Figure 4A it can be seen that there is a sharp increase in the curve of RMSD values during the initial heating stage of 20 ps, indicating that significant structural changes occur in the heating stage. A slow increase in the RMSD curve during the entire equilibrium phase indicates a relatively stable approach to the final structure.

Figure 4

Using the initial and final conformations of Cyt1A, we also define RMSD as a function of residue number j as below:

$$RMSD(j) = \sqrt{\frac{1}{N_j} \sum_{i=1}^{N_j} [(x_i^F - x_i^I)^2 + (y_i^F - y_i^I)^2 + (z_i^F - z_i^I)^2]} \quad , \quad (2)$$

where $j = 1, 2, \dots, N_R$, N_R is the number of residues, the superscript F denotes the final conformation at the end of the quenching phase of the MD simulation, I denotes the initial conformation at the start of MD, and N_j is the number of atoms in the j^{th} residue. For Cyt1A, $N_R = 249$, and the values of $RMSD(j)$ with $j = 1, 2, \dots, N_R$ are reported in Figure 4B. From this plot we can see that the MD simulation has caused significant structure changes in some residues of Cyt1A, even though the overall displacement by MD is rather small. According to the figure, the significant structure changes mainly occur on the first 50 residues (i.e., the N-terminal tail of the molecule) with displacements of more than 5 Å. For illustrations, comparisons of the initial and final conformations of four structure segments — (1) residues 20 – 40, (2) residues 102 – 128, (3) residues 153 – 173, and (4) residues 229 – 249 — are presented in Figure 5.

Figure 5

While RMSD only indicates how different the final MD structure is from the initial one, the root mean square fluctuations (RMSF) can measure the molecular fluctuations about the time averaged structure and indicate the flexibility of the

molecule. We calculated RMSF for each residue of Cyt1A by:

$$RMSF(j) = \sqrt{\frac{1}{N_j M} \sum_{i=1}^{N_j} \sum_{k=1}^M [(x_{i,t_k} - \langle x_i \rangle)^2 + (y_{i,t_k} - \langle y_i \rangle)^2 + (z_{i,t_k} - \langle z_i \rangle)^2]} \quad , \quad (3)$$

where $j = 1, 2, \dots, N_R$, M is the total number of sampling conformations in the equilibration phase of the MD simulation, $t_k = 20 + k\tau$ with $\tau = 0.2$ ps, $(x_{it_k}, y_{it_k}, z_{it_k})$ and $(\langle x_i \rangle, \langle y_i \rangle, \langle z_i \rangle)$ denotes the position vector of atom i at timestep t_k and the averaged position vector of atom i over the M time steps, respectively. The units of RMSF are Angstroms. Here the conformation data came from the equilibrium stage in the MD simulation with $M = 2000$. The calculated results were displayed in Figure 6.

From Figure 6 we see that the most flexible parts of Cyt1A are the N and C termini, but within the amino acid sequence there are also regions with large RMSF values. Residues with RMSF larger than 1.8 \AA are listed in Table 2. They were also visualized in cyan color on the three dimensional molecular structure of Cyt1A in Figure 7. As depicted in Figure 7, the highly dynamic, flexible parts are on the top and bottom of the Cyt1A molecule. This certainly is reasonable, since the loops connecting β strands in the Cyt1As central β sheet are located there. Interestingly, majority of the mutations that render the toxin inactive [15] are located in the top part of the molecule, which led to the hypothesis that this region of the molecule is important for binding of Cyt1A to the lipid or for the cytolytic action of the toxin in general [1]. Our results support that hypothesis.

Figure 6

Table 2

Figure 7

3.4 Structure of a mutated Cyt1A

Ward et al. [15] produced several mutated forms of Cyt1A, in which several single amino acid residues were replaced by a small non-polar amino acid alanine respectively. The mutated proteins were then tested for toxicity and lipid binding. It is not easy to interpret those results, since the mutated toxin molecules may lose their activity for two possible reasons. First, the mutated amino acid residue may be required for specific docking of the toxin on the lipid membrane or for interactions with

other toxin molecules during formation of pores or aggregates in the membrane; when that residue is missing, the toxin cannot bind or assemble in the normal manner. The second possibility is that replacing the given amino acid residue with alanine may result in a conformation change in the toxin that renders it inactive. According to Ward et al., replacement of Lys163 with Ala resulted in the loss of activity [15].

To address this question we performed the mutation *in silico* by replacing Lys163 with Ala based on the 3D molecular structure of Cyt1A generated from our MD simulations. An initial structure of the mutated Cyt1A was produced by Swiss-PdbViewer. This initial structure was then refined by molecular potential energy minimization in solution with CHARMM.

Figure 8 shows the effect of such a replacement on the local conformation of Cyt1A after energy minimization. It is trivial that the long side chain of the Lys residue is missing in the mutated toxin, but it is less trivial that the replacement did not affect conformation in the close vicinity of the residue 163. We offer two possible explanations. First, the residue in question is on the surface of the toxin and so packing constraints of the protein interior do not play a role. Second, it is possible that the mere energy minimization cannot reveal conformation changes caused by the mutation; the changes may require some time to spread within the toxin structure. The latter possibility will be tested in further MD simulations, which should reveal the entropic cost due to the unfavorable exposure of the non-polar Ala to the solvent.

Figure 8

4 Conclusions

In the absence of experimental structure determined by, e.g., X-ray diffraction or NMR, we have obtained a stable molecular structure of Cyt1A by using the homology modeling and molecular potential energy minimization. Starting from the predicted toxin structure, we carried out the MD simulations to Cyt1A in solution for 960 ps using CHARMM. Our simulations validated and refined the previous predicted structure of Cyt1A in solution. We also present initial attempts to study the effect on

Cyt1A structure of known experimental mutations that render the toxin inactive [15]. While this question requires further work, our simulations have yielded some interesting insights. An analysis of the MD conformation data led to the identification of the regions in Cyt1A that exhibit a higher than average flexibility. This characteristic makes those regions the prime candidate for localization of conformation changes during binding to the lipid membrane and the initial stages of the toxin-induced cytolysis. This finding thus may be relevant for elucidation of the toxin's mode of action.

Acknowledgments

This research was supported by the National Science Foundation (DMS-0241236) and, in part, by the Cooperative State Research, Education, and Extension Service, US Department of Agriculture (agreement number 2001-35302-1011138), and the Graduate School Research Committee award (grant number 343267-101-4) of the University of Wisconsin-Milwaukee.

References

- [1] Butko, P., Cytolytic toxin Cyt1A and its mechanism of membrane damage: data and hypotheses. *Appl. Environ. Microbiol.* **2003**, *69* (5), 2415-2422.
- [2] Wu, D., Johnson, J.J., and Federici, B.A., Synergism of mosquitocidal toxicity between CytA and CryIVD proteins using inclusions produced from cloned genes of *Bacillus thuringiensis*. *Mol. Microbiol.* **1994**, *13* (6), 965-972.
- [3] Wirth, M.C., Walton, W.E., and Federici, B.A., Cyt1A from *Bacillus thuringiensis* synergizes activity of *Bacillus sphaericus* against *Aedes aegypti*(Diptera: Culicidae). *Appl. Environ. Microbiol.* **2000**, *66* (3), 1093-1097.

- [4] Butko, P., et al., Membrane permeabilization induced by cytolytic delta-endotoxin CytA from *Bacillus thuringiensis* var. *israelensis*. *Biochemistry* **1996**, *35 (35)*, 11355-11360.
- [5] Knowles, B.H., et al., A cytolytic delta-endotoxin from *Bacillus thuringiensis* var. *israelensis* forms cation-selective channels in planar lipid bilayers. *FEBS Lett.* **1989**, *244 (2)*, 259-262.
- [6] Promdonkoy, B., and Ellar, D.J., Membrane pore architecture of a cytolytic toxin from *Bacillus thuringiensis*. *Biochem. J.* **2000**, *350 Pt 1*, 275-282.
- [7] Manceva, S.D., et al., A Detergent-Like Mechanism of Action of the Cytolytic Toxin Cyt1A from *Bacillus thuringiensis* var. *israelensis* , 2004.
- [8] Ellar, D.J., The insecticidal proteins of *Bacillus thuringiensis*, in BT100: A celebration of the 100th anniversary of the discovery of *Bacillus thuringiensis*, M. Ohba, et al., Editors. *Kurume, Japan* **2002**, 179-189.
- [9] Butko, P., et al., Interaction of the delta-endotoxin CytA from *Bacillus thuringiensis* var. *israelensis* with lipid membranes. *Biochemistry* **1997**, *36 (42)*, 12862-12868.
- [10] Li, J., Koni, P.A., and Ellar, D.J., Structure of the mosquitocidal delta-endotoxin CytB from *Bacillus thuringiensis* sp. *kyushuensis* and implications for membrane pore formation. *J. Mol. Biol.* **1996**, *257 (1)*, 129-152.
- [11] Brooks, B.R., Bruccoleri, R.E., Olafson, B.D., States, D.J., Swaminathan, S., and Karplus, M., CHARMM: A Program for Macromolecular Energy, Minimization, and Dynamics Calculations. *J. Comp. Chem.* **1983**, *4*, 187-217.
- [12] MacKerell, A.D. Jr., Brooks, B., Brooks, C.L. III, Nilsson, L., Roux, B., Won, Y., and Karplus, M., CHARMM: The Energy Function and Its Parameterization with an Overview of the Program. *The Encyclopedia of Computational Chemistry* **1998**, *1*, 271-277.

- [13] Schwede, T., Kopp, J., Guex, N., and Peitsch M.C. SWISS-MODEL: an automated protein homology-modeling server. *Nucleic Acids Research* **2003**, *31*, 3381-3385.
- [14] Manceva, S.D., Pusztai-Carey, M. and Butko, P., Effect of pH and Ionic Strength on the Cytolytic Toxin Cyt1A: A fluorescence Spectroscopy Study. *Biochim. Biophys. Acta.* **2004**, *1699*, 123-130.
- [15] Ward, E.S., Ellar, D.J., and Chilcott, C.N., Single amino acid changes in the *Bacillus thuringiensis* var. *israelensis* delta-endotoxin affect the toxicity and expression of the protein. *J. Mol. Biol.* **1988**, *202*, 527-535

List of Figures

1	(A) Energy evolution of the Cyt1A-water system in the heating, equilibration and quenching stages of MD simulations. (B) Enlarged view of the total energy.	15
2	(A) The initial structure of Cyt1A generated from Swiss-Model, based on the crystal structure of Cyt2A. (B) The refined structure of Cyt1A by molecular potential energy minimizations. (C) A comparison of the initial structures (gray) with the refined ones (blue).	15
3	Comparison of the three secondary structure elements of Cyt1A generated by Swiss-Model, energy minimization, and MD simulation, respectively. Here the residues in beta strands are denoted by stars and the ones in alpha helices by circles.	16
4	(A) The values of $RMSD$ of Cyt1A as a function of time steps. (B) The values of $RMSD$ of Cyt1A as a function of residue numbers. Here, $RMSD(t)$ and $RMSD(j)$ are defined in (1) and (2), respectively. .	16
5	Comparison of the backbone structures of four segments of Cyt1A at the starting of MD (gray) with that at the end of MD (blue). Here, (A) for segment of residues 20 – 40 (N-terminal), (B) for segment of residues 102 – 128, (C) for segment of residues 153 – 173, and (D) for segment of residues 229 – 249.	17
6	Root mean square fluctuations (RMSF) as a function of residue number.	17
7	Relative flexibility of amino acid residues in Cyt1A predicted by MD. Here residues with RMSF values larger than 1.8 Å are colored cyan. .	18
8	The effect of replacement of Lys 163 by Ala on the structure of Cyt1A after molecular potential energy minimization. Here (A) for the structure with Lys and (B) for the structure with Ala.	18

List of Tables

1	The energy changes ΔE of Cyt1A produced by the molecular potential energy minimizations.	18
2	The residues with RMSF values larger than 1.8 Å.	19

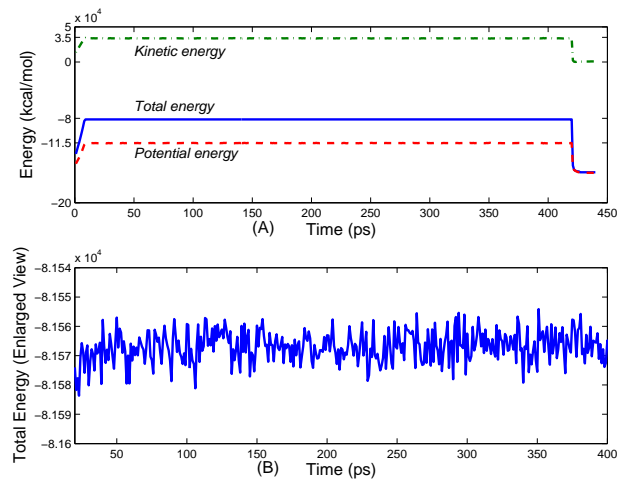


Figure 1: (A) Energy evolution of the Cyt1A-water system in the heating, equilibration and quenching stages of MD simulations. (B) Enlarged view of the total energy.

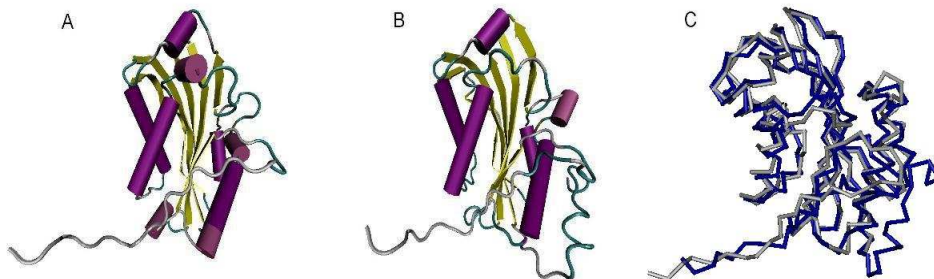


Figure 2: (A) The initial structure of Cyt1A generated from Swiss-Model, based on the crystal structure of Cyt2A. (B) The refined structure of Cyt1A by molecular potential energy minimizations. (C) A comparison of the initial structures (gray) with the refined ones (blue).

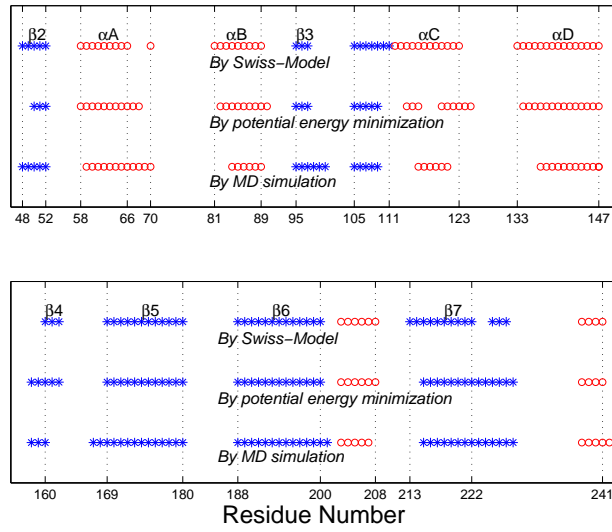


Figure 3: Comparison of the three secondary structure elements of Cyt1A generated by Swiss-Model, energy minimization, and MD simulation, respectively. Here the residues in beta strands are denoted by stars and the ones in alpha helices by circles.

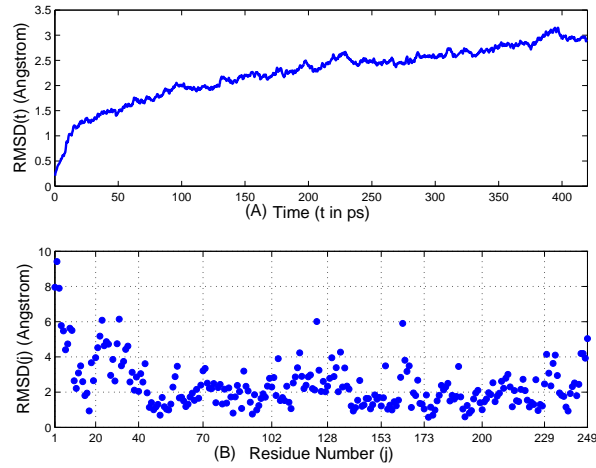


Figure 4: (A) The values of $RMSD$ of Cyt1A as a function of time steps. (B) The values of $RMSD$ of Cyt1A as a function of residue numbers. Here, $RMSD(t)$ and $RMSD(j)$ are defined in (1) and (2), respectively.

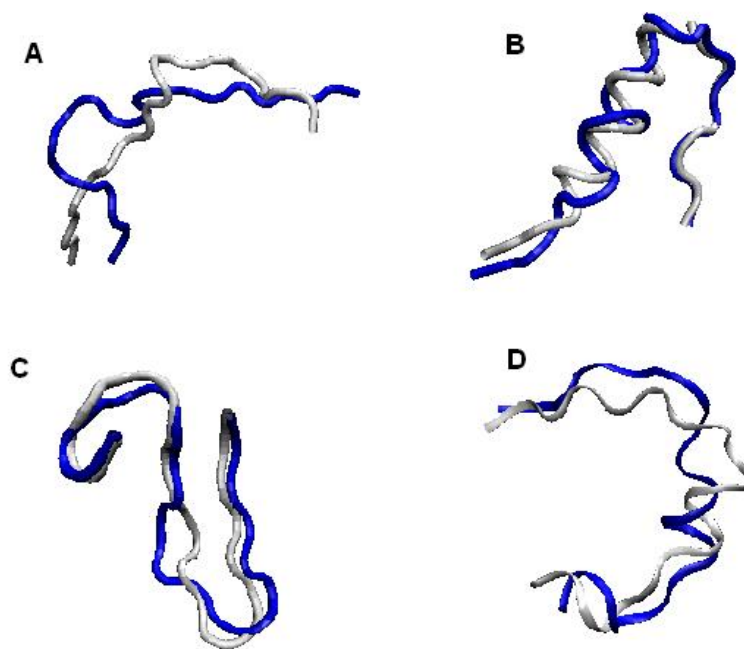


Figure 5: Comparison of the backbone structures of four segments of Cyt1A at the starting of MD (gray) with that at the end of MD (blue). Here, (A) for segment of residues 20 – 40 (N-terminal), (B) for segment of residues 102 – 128, (C) for segment of residues 153 – 173, and (D) for segment of residues 229 – 249.

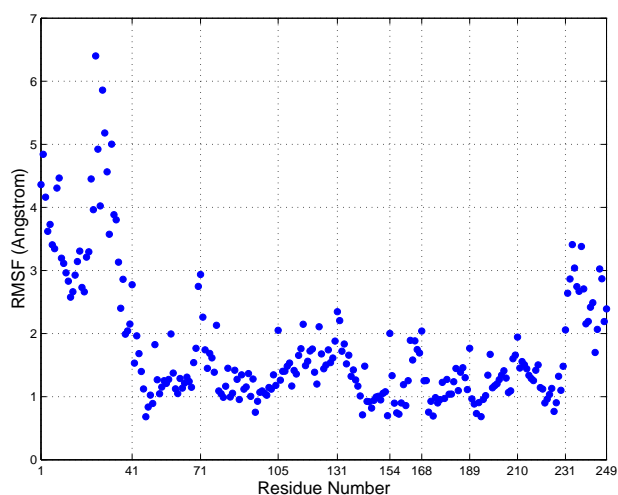


Figure 6: Root mean square fluctuations (RMSF) as a function of residue number.

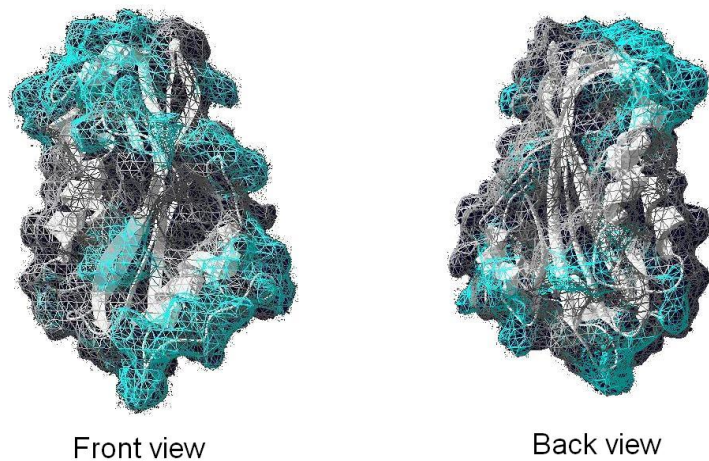


Figure 7: Relative flexibility of amino acid residues in Cyt1A predicted by MD. Here residues with RMSF values larger than 1.8 Å are colored cyan.

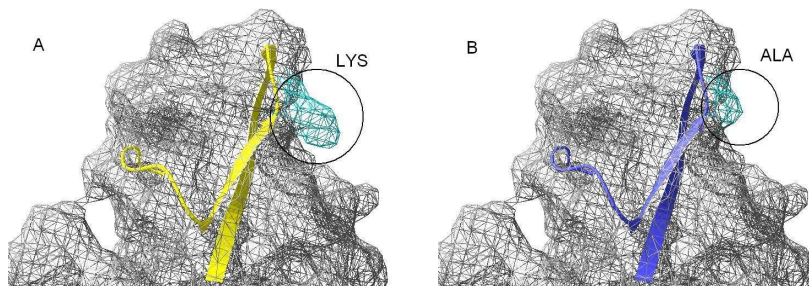


Figure 8: The effect of replacement of Lys 163 by Ala on the structure of Cyt1A after molecular potential energy minimization. Here (A) for the structure with Lys and (B) for the structure with Ala.

Table 1: The energy changes ΔE of Cyt1A produced by the molecular potential energy minimizations.

	ΔE in Vacuum (<i>kcal/mol</i>)	ΔE in Water (<i>kcal/mol</i>)
Bond Length Energy	-194.1	4499.0
Van der Waals Energy	-270.6	31932.3
Electrostatic Energy	-1487.2	-100563.1
Total Energy	-1951.9	-64131.8

Table 2: The residues with RMSF values larger than 1.8 Å.

Residue number	1	2	3	4	5	6	7	8	9	10
RMSF (Å)	4.36	4.84	4.16	3.62	3.72	3.41	3.35	4.31	4.47	3.20
Residue number	11	12	13	14	15	16	17	18	19	20
RMSF (Å)	3.11	2.96	2.83	2.58	2.66	2.93	3.14	3.31	2.73	2.66
Residue number	21	22	23	24	25	26	27	28	29	30
RMSF (Å)	3.12	3.30	4.45	3.96	6.40	4.92	4.02	5.86	5.18	4.56
Residue number	31	32	33	34	35	36	37	38	39	40
RMSF (Å)	3.57	5.00	3.88	3.80	3.13	2.40	2.86	1.99	2.04	2.15
Residue number	41	43	51	58	70	71	72	78	105	116
RMSF (Å)	2.77	1.96	1.83	1.99	2.74	2.94	2.26	2.13	2.05	2.15
Residue number	123	130	131	132	134	154	163	165	168	210
RMSF (Å)	2.11	1.88	2.35	2.21	1.83	2.00	1.89	1.88	2.04	1.94
Residue number	231	232	233	234	235	236	237	238	239	240
RMSF (Å)	2.06	2.64	2.87	3.41	3.04	2.74	2.67	3.38	2.70	2.15
Residue number	241	242	243	245	246	247	248	249		
RMSF (Å)	2.19	2.42	2.49	2.07	3.02	2.87	2.19	2.39		